Pergamon

Int. J. Solids Structures Vol. 32, No. 11, pp. 1585–1594, 1995

0020–7683/95 $9.50 + .00

0020–7683(94)00193–6

DYNAMIC ANALYSIS OF ARCH BRIDGES UNDER TRAVELLING LOADS

P. K. CHATTERJEE
Structural Engineering Research Centre, 19, Kamla Nehru Nagar, P.O. Box 10, Ghaziabad 201001, India

and

T. K. DATTA
Civil Engineering Department, Indian Institute of Technology, Delhi, Hauz Khas, New Delhi 110016, India

(*Received* 2 *October* 1993; *in revised form* 5 *August* 1994)

Abstract—A dynamic analysis of arch bridges traversed by a single moving load is presented using a mixed approach in which the advantages of continuum and lumped mass methods have been combined. The bridge deck is idealized by a flat plate supported by struts of equal stiffness. The applicability of the method is studied by comparing the results with those obtained by the lumped mass method. The results indicate that for a relatively stiff arch supporting a flexible deck, the proposed and the lumped mass methods show good agreement. The dynamic behaviour of the bridge under some important parametric variations is also presented.

1. INTRODUCTION

Arch bridges are constructed for short to medium spans. In the past, arches were provided with heavy cross-sectional area with solid filled over the arch up to the bridge pavement. Aesthetics dictate a relatively slender arch supporting a flexible deck through the struts, and such are constructed.

Compared to other types of bridges, the dynamics of arch bridges are given less attention for theoretical studies. Lee and Wilson (1989) obtained the natural frequencies and mode shapes for parabolic, sinusoidal and elliptic arches with distributed mass for the arch and also gave the experimental validations for the lowest four predicted frequencies and mode shapes for a parabolic arch. Raithel and Franciosi (1984) used the Lagrange approach with lumped masses for finding the frequencies and modes of vibration for any arbitrary arch. Nair (1986) proposed a simple method to calculate the buckling loads, natural frequencies and corresponding mode shapes for arches and tied arches (which resemble an arch bridge) using the lumped mass approach. For very steep arches, he showed that the simplifying assumptions could result in significant errors in predicting the buckling loads and frequencies. Recently, Dusseau and Wen (1989) investigated the effect of seismic forces on three different steel arch bridges. A finite element model for each bridge was used to calculate the dynamic response of the bridge due to artificial ground motions applied separately along three directions. Their results indicate that the seismic response to vertical bridge motion is generally lower than that due to lateral and longitudinal motions.

So far as the dynamics of arch bridges due to moving loads (idealizing the vehicles) are concerned, the literature on the subject is surprisingly meagre. The continuum approach used in this paper is similar to that of the response analysis of elastically supported beams to moving loads, an excellent review of which is given in the ASCE paper (1985). The applicability of the proposed method is demonstrated by comparing its results with those obtained by the lumped mass method. Using the proposed method of analysis, a parametric study is conducted to investigate the dynamic behaviour of arch bridges under moving loads.

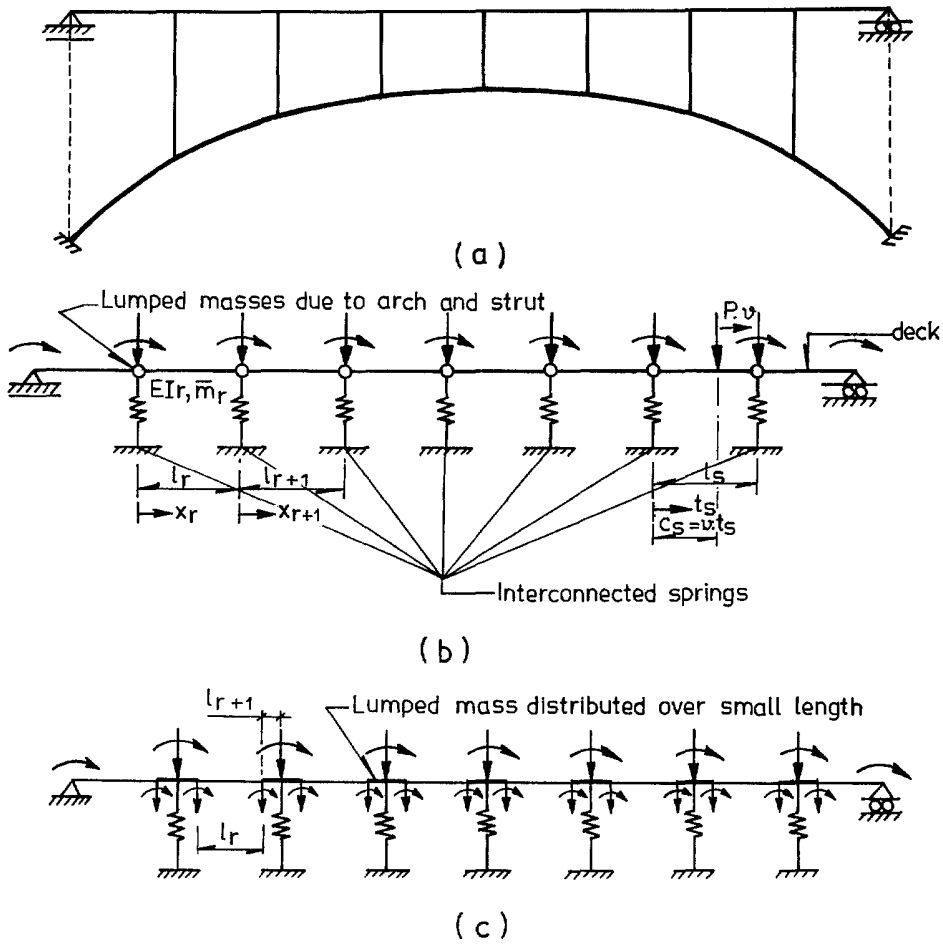

Fig. 1(a). Idealized arch bridge; (b) continuum model of arch bridge with lumped masses; (c) continuum model of arch bridge with distributed masses.

2. ASSUMPTIONS

The following assumptions are made for the formulation of the problem.

1. The bridge deck is treated as a beam having uniform flexural rigidity and uniform mass per unit length for any segment of the beam between two struts; these two characteristics may change from segment to segment.
2. The vehicle is represented by a single constant vertical load P moving at a constant speed v along the centre line of the bridge deck so that a two-dimensional idealization of the bridge is possible.
3. The movement of the arch including the axial shortening of the struts with respect to time is assumed to be quasi-static, so that the deck vibration can be separated from the arch vibration.

3. RESPONSE OF CONTINUOUS BEAM UNDER MOVING LOAD

The governing equation of motion for any segment r [Fig. 1(b)] of the idealized beam (neglecting shear deformation and rotatory inertia) may be written as

$$EI_r \frac{\partial^4 W(x_r, t)}{\partial x_r^4} + 2\xi\omega\bar{m}_r \frac{\partial W(x_r, t)}{\partial t} + \bar{m}_r \frac{\partial^2 W(x_r, t)}{\partial t^2} = p(x_r, t) \tag{1}$$

in which $W(x_r, t)$ and $p(x_r, t)$ are the dynamic deflection of the beam and the value of load

acting on the beam at x_r and at any time t; ξ is the damping ratio; ω is the natural frequency of the bridge; $\bar{m}_r$ and EI_r are the mass/unit length and flexural rigidity of the beam segment.

The expression for the nth mode shape of the rth beam segment is given by

$$\phi_{nr}(x_r) = A_{nr}\cos\beta_{nr}x_r + B_{nr}\sin\beta_{nr}x_r + C_{nr}\cosh\beta_{nr}X_r + D_{nr}\sinh\beta_{nr}x_r \tag{2}$$

where A_{nr}, etc. are integration constants expressed in terms of the nth natural frequency ω_n and

$$\beta_{nr} = \bar{m}_r\omega_n^2/EI_r \tag{3}$$

where n and r are two integers.

Utilizing (2), the relation between the end force vector $\{F\}_r$ (shear force and bending moment) and end displacement vector $\{X\}_r$ (vertical displacement and slope) may be written as

$$\{F\}_r = [K]_r\{X\}_r \tag{4}$$

where $[K]_r$ is called the "dynamic stiffness matrix" (of order 4×4) for the rth beam segment. The end displacements $\{X\}_r$ may also be related to the integration constant vector $\{C\}_r$ as

$$\{C\}_r = [R]_r\{X\}_r \tag{5}$$

where $[R]_r$ is called the "integration constant matrix" for the rth segment. The explicit expressions for the matrices $[K]_r$ and $[R]_r$ are given by Hayashikawa and Watanabe (1981). Assembling the individual dynamic stiffness matrix $[K]_r$ ($r = 1$–N, where N is the total number of segments) to form the global dynamic stiffness matrix $[K]$, the free vibration condition of the beam is given by

$$[K]\{U\} = \{0\} \tag{6}$$

where $\{U\}$ is the unknown end displacement vector for the entire beam. Equation (6) leads to.

$$\det[K] = 0. \tag{7}$$

The natural frequencies of the bridge can be obtained from the solution of (7); the mode shapes can be found through the use of eqns (6), (5) and (2).

Using the mode superposition technique, the dynamic deflection of the beam and the load on the beam are expressed as

$$W(x_r, t_s) = \sum_{n=1}^{\infty}\phi_{nr}(x_r)T_{ns}(t_s) \tag{8}$$

$$p(x_r, t_s) = \sum_{n=1}^{\infty}\phi_{nr}(x_r)q_n(t_s) \tag{9}$$

where $T_{ns}(t_s)$ is the displacement function in generalized coordinate, t_s is measured from the instant when the load is just on the left of sth (loaded) span, and

$$q_n = (P/M_n^2)\,\phi_{ns}(v\cdot t_s), \tag{10}$$

in which

$$M_n^2 = \sum_{r=1}^{N} \int_0^{l_r} \phi_{nr}(x_r) \mathrm{d}x_r, \tag{11}$$

where l_r is the length of the rth segment, P and v are the magnitude and speed of the load. Substituting (8) and (9) into (1) and solving the resulting equation, $T_{ns}(t_s)$ can be obtained by a few closed form recursive expressions as given by Chatterjee *et al.* (1994).

4. RESPONSE ANALYSIS FOR THE ARCH BRIDGE

The idealized bridge is shown in Fig. 1(a). Since the dynamic response of the deck is of main interest, the equivalent continuum model of the bridge is shown in Fig. 1(b). The effect of the struts is considered by replacing the struts by a number of interconnected springs located at the deck–strut joints. The coupled spring stiffness matrix is obtained from the condensation of the static stiffness matrix of the bridge [Fig. 1(a)] to the vertical degrees of freedom corresponding to the deck–strut joints. The spring stiffness matrix is properly superimposed on the global dynamic stiffness matrix $[K]$ of the beam (i.e. corresponding to the vertical degrees of freedom of the beam) before using the free vibration condition given by (7).

To consider the inertia effect of the struts and the arch along with the deck, the mass of the struts and the appropriate portion of the mass of the arch are lumped at the beam joints as shown in Fig. 1(b). In order to make use of the advantages of continuum analysis as described in the preceding section, these lumped masses at the nodes are distributed over small lengths (typically $s/50$, where s is the span between two struts) as indicated in Fig. 1(c) and a continuum analysis is performed (method 2). This technique increases the number of dynamic degrees of freedom since the number of spans (L_r, L_{r+1}, etc.) to be considered in the continuum analysis increases, and requires more computational time. In order to reduce the computational effort, another approach is presented (method 3) in which the inertia effects of these lumped masses are considered in the dynamic analysis in an approximate manner by subtracting from the diagonal elements of the overall dynamic stiffness matrix $[K]$ of the beam (described in the previous section) the quantities $m_i\omega^2$, where m_i is the magnitude of the ith lumped mass at the beam–strut joint [Fig. 1(b)]. This approach does not strictly satisfy the condition of orthogonality of mode shapes for the continuum solution presented in Section 3 (Wu and Lin, 1990). The validity of the proposed methods (methods 2 and 3) is investigated by comparing their results with those of lumped mass approach (method 1). In the lumped mass approach, the masses of the bridge members (i.e. arch, struts and deck) are lumped at the deck–strut and the arch–strut joints. Two additional lumped mass points over the deck in between the struts are also considered for better simulation of the deck behaviour. The problem is then converted into a multi-degree of freedom lumped mass system subjected to a vertical concentrated moving load along the deck. The response is obtained by numerically integrating the matrix equations of motion by Newmark's beta method (Bathe and Wilson, 1987). The efficiency of the solution is enhanced by the use of normal mode theory.

5. NUMERICAL EXAMPLES

The following properties are considered for the arch bridge shown in Fig. 1(a): span of the bridge, $L = 80.0$ m; arch profile is assumed to be parabolic with height of crown = 12.0 m; height of deck above the crown = 2.5 m; cross-sections of the arch and the struts are considered to be of solid rectangular sections with the same width of 6.0 m; thickness of the arch section is considered uniform at 1.0 m; $E = 2.85 \times 10^{11}$ N/m^2. Other properties of the bridge are defined automatically once the values of following non-dimensional parameters are prescribed:

Table 1. Natural frequencies (rad/s) and DAF for arch bridge $\delta_1 = 0.5$, $\delta_2 = 0.7$, $\delta_3 = 8.0$, $\delta_4 = 0.6$

Mode	Lumped mass approach	Continuum approach	
		Distributed masses over small lengths	Concentrated masses at joints
1	16.16	18.20	18.88
2	17.75	20.12	20.99
3	27.30	30.90	31.56
4	33.03	38.78	38.52
5	37.75	42.89	43.32
6	49.29	57.21	56.33
7	63.66	73.10	71.73
8	102.60	90.23	89.63
9	114.13	95.99	94.32
10	121.07	107.22	105.73
DAF	1.070	1.060	1.062

$$\delta_1 = I_d/I_a \tag{12a}$$

$$\delta_2 = A_d/A_a \tag{12b}$$

$$\delta_3 = (EA_s/l_s)/(EA_a/L) \tag{12c}$$

$$\delta_4 = \bar{m}_d/\bar{m}_a \tag{12d}$$

where I, A and m indicate the moment of inertia, cross-sectional area and mass per unit length of any member under consideration, and the subscripts a, d and s refer to the arch, deck and struts, respectively. For simplicity of the numerical analysis, the values of (EA_s/l_s) for all struts are kept same and the arch section is assumed uniform throughout.

The fundamental frequency of the arch without the deck is computed as 51.9 rad/s (for $\delta_1 = \delta_2 = 0.7$, $\delta_3 = 4.0$ and $\delta_4 = 1.0$). Also, the frequency of the deck only with simply supported ends is obtained as 4.8 rad/s. The ratio of arch to deck frequency is thus determined as 11.5, which is large enough to assume that the deck vibration can be separated from the arch vibration (assumption number 3).

The speed parameter (α) is defined here as

$$\alpha = \beta_{11} v/\omega_1 \tag{13}$$

where β_{11} corresponds to (3) and ω_1 is the fundamental frequency of vibration of the arch bridge.

Table 1 shows the first ten natural frequencies obtained by these methods. It is found that for lower modes of vibration, the continuum approach generally gives higher values of natural frequencies.

Table 1 also shows the values of dynamic amplification factors (DAF, defined as the ratio of maximum dynamic response and maximum static response at a point) for deflection of the deck at the middle of the fourth and fifth struts (for $v = 20.0$ m/sec, $\xi = 0$ and $P = 1.0 \times 10^5$ N). The values of DAF for method 2 and method 3 are practically the same. Thus, method 3, which does not strictly satisfy the conditions of orthogonality of mode shapes for continuum solution (Wu and Lin, 1990), can be used for all practical purposes.

Tables 2(a)–(d) show the first ten natural frequencies (in rad/s) of the bridge for different combinations of the parameters δ_1 to δ_4.

For a rigid arch supporting a relatively much more flexible bridge deck [i.e. δ_2 and δ_3 very low in (12a,c)], the lumped and continuum approaches provide nearly the same results. This is due to the fact that the vibrations of the deck and the arch are separated by a relatively small stiffness of the struts (which is replaced by very flexible springs). Therefore, the deck behaves like a simply supported beam. In this case, the first few frequencies for both methods are nearly the same and for these frequencies, the modes of vibration of the bridge are predominantly the deck mode of vibration.

Table 2(a). Variation of natural frequencies (rad/s) with δ_1; $\delta_2 = 0.4$, $\delta_3 = 8.0$, $\delta_4 = 0.6$

Mode	Continuum approach			Lumped mass approach		
	$\delta_1 = 0.3$	$\delta_1 = 0.5$	$\delta_1 = 0.7$	$\delta_1 = 0.3$	$\delta_1 = 0.5$	$\delta_1 = 0.7$
1	17.81	18.70	19.28	15.26	16.01	16.50
2	19.92	20.98	21.84	16.90	17.74	18.40
3	29.81	31.55	33.05	25.92	27.29	28.48
4	38.06	38.51	38.71	32.57	33.02	33.26
5	40.79	43.31	45.70	35.84	37.75	39.55
6	52.14	56.32	60.07	46.10	49.28	52.18
7	65.56	71.73	76.93	59.23	63.66	67.69
8	69.42	89.63	106.05	83.28	102.58	118.20
9	73.78	94.32	111.43	93.96	114.09	130.20
10	82.09	105.73	125.00	97.92	121.04	139.66

Table 2(b). Variation of natural frequencies (rad/s) with δ_2; $\delta_1 = 0.5$, $\delta_3 = 8.0$, $\delta_4 = 0.6$

Mode	Continuum approach			Lumped mass approach		
	$\delta_2 = 0.4$	$\delta_2 = 0.7$	$\delta_2 = 1.0$	$\delta_2 = 0.4$	$\delta_2 = 0.7$	$\delta_2 = 1.0$
1	18.70	18.88	18.95	16.01	16.16	16.23
2	20.98	20.99	21.00	17.74	17.75	17.75
3	31.55	31.56	31.57	27.29	27.30	27.30
4	38.51	38.52	38.53	33.02	33.03	33.04
5	43.31	43.32	43.32	37.75	37.75	37.76
6	56.32	56.33	56.33	49.28	49.29	49.29
7	71.73	71.73	71.73	63.66	63.66	63.66
8	89.63	89.63	89.63	102.58	102.60	102.61
9	94.32	94.32	94.32	114.09	114.20	114.13
10	105.73	105.73	105.73	121.04	121.07	121.08

Table 2(c). Variation of natural frequencies (rad/s) with δ_3; $\delta_1 = 0.5$, $\delta_2 = 0.8$, $\delta_4 = 0.8$

Mode	Continuum approach			Lumped mass approach		
	$\delta_3 = 3.0$	$\delta_3 = 6.5$	$\delta_3 = 10.0$	$\delta_3 = 3.0$	$\delta_3 = 6.5$	$\delta_3 = 10.0$
1	5.61	8.47	11.08	4.38	6.79	9.09
2	9.24	10.23	11.29	7.19	8.16	9.20
3	15.68	15.75	16.32	12.29	12.75	13.51
4	22.20	21.73	22.01	17.44	17.59	18.35
5	29.83	28.70	28.26	23.79	23.52	23.77
6	36.54	36.00	35.48	30.11	30.19	29.65
7	38.81	37.90	36.65	31.42	30.67	30.51
8	39.33	38.81	38.81	39.28	42.59	47.26
9	41.63	41.39	41.26	43.55	47.33	53.46
10	46.29	46.13	46.03	49.85	51.73	55.64

Table 2(d). Variation of natural frequencies (rad/s) with δ_4; $\delta_1 = 0.5$, $\delta_2 = 0.6$, $\delta_3 = 8.0$

Mode	Continuum approach			Lumped mass approach		
	$\delta_4 = 1.0$	$\delta_4 = 0.8$	$\delta_4 = 0.6$	$\delta_4 = 1.0$	$\delta_4 = 0.8$	$\delta_4 = 0.6$
1	18.51	18.67	18.84	14.70	15.36	16.13
2	20.61	20.80	20.99	16.11	16.87	17.74
3	31.04	31.30	31.56	25.06	26.11	27.30
4	37.79	38.16	38.52	29.98	31.40	33.03
5	42.56	42.94	43.31	34.71	36.15	37.75
6	55.11	55.75	56.32	45.26	47.17	49.29
7	68.30	70.64	71.73	58.80	61.14	63.66
8	69.42	77.62	89.63	79.81	89.06	102.60
9	75.87	82.49	94.32	89.94	99.67	114.11
10	82.94	92.08	105.73	96.39	106.33	121.06

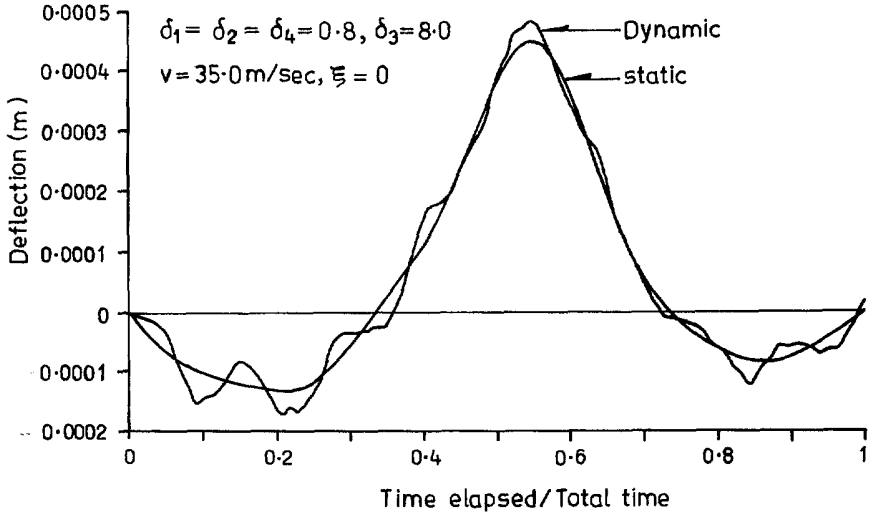

Fig. 2. Influence lines for deflection of deck.

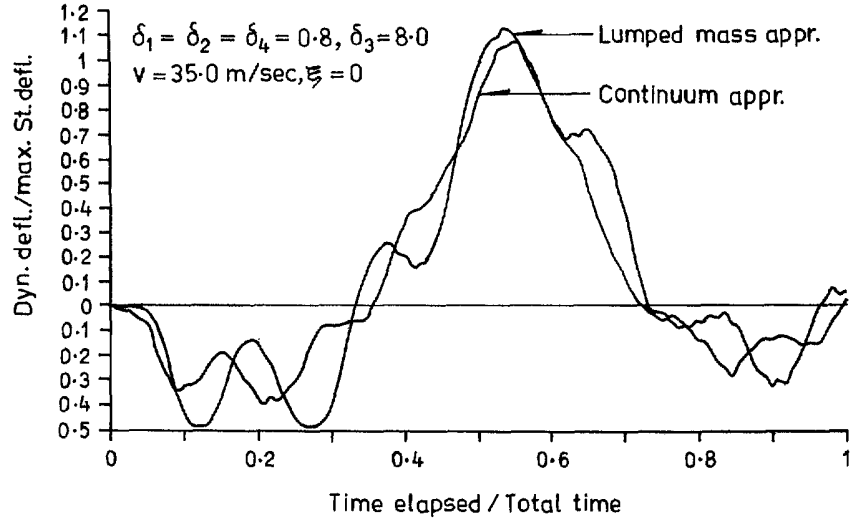

Fig. 3. Comparison of influence lines between continuum and lumped mass method.

For a relatively flexible arch, the difference between the results of lumped mass and continuum approaches vary by different degrees. Generally, the differences between the first three or four natural frequencies are pronounced. It is generally seen that the differences between the natural frequencies for the 6th–10th mode of vibration vary between 5 and 20%, while for the first three frequencies the differences are large (from 20 to 40%). Generally, for higher flexural and axial rigidities of the arch, lower axial rigidity of the struts and relatively higher mass of the deck, these differences become less.

Figure 2 shows the influence lines for static and dynamic deflection ($v = 35.0$ m/s, $\xi = 0$) at the one-third point between the fourth and fifth struts for the case when $\delta_1 = 0.8$, $\delta_2 = 0.8$, $\delta_3 = 8.0$ and $\delta_4 = 0.8$. Figure 3 compares the influence lines for continuum and lumped mass approaches for the same problem. The dynamic amplification factors obtained for the two cases are 1.074 and 1.124, respectively.

The dynamic amplification factors obtained by the two approaches are compared in Figs 4(a)–(c) for different combinations of the parameters δ_1–δ_4. For certain speeds and specific combinations of δ_1–δ_4, the DAF obtained by the two approaches agree well with each other. For other combinations, different degrees of variation of the results are observed for the two approaches. Differences are mainly due to the difference in the first three or

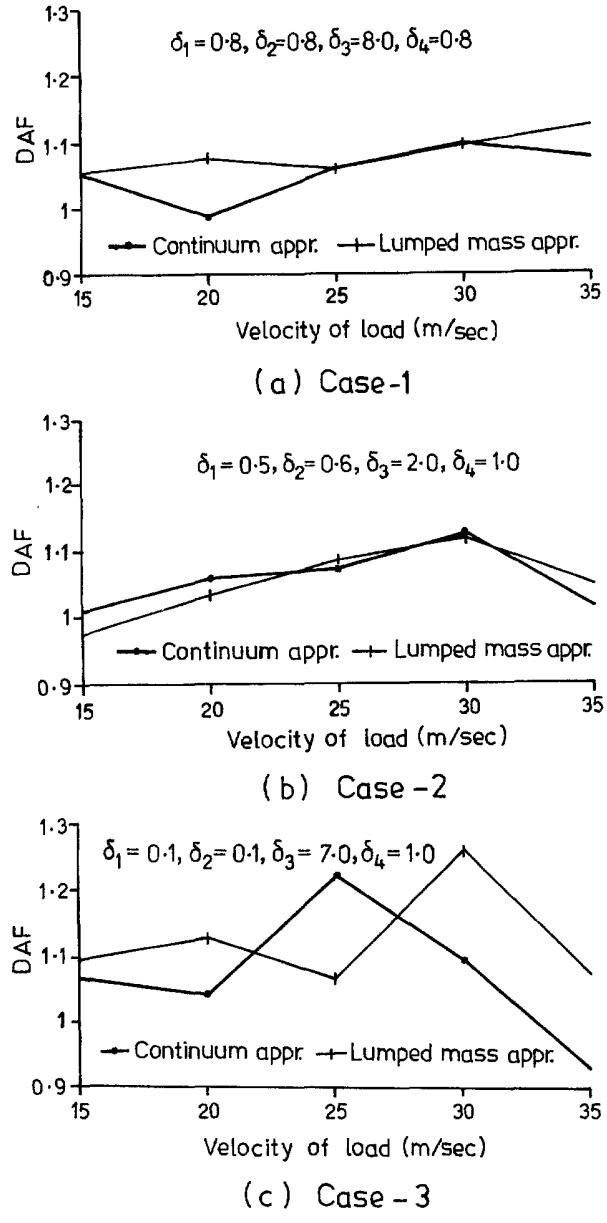

Fig. 4. Comparison of DAFs for continuum and lumped mass method.

four natural frequencies obtained by the two methods and the participation of vibration of the arch in the overall vertical mode of vibration of the bridge. Note that the continuum approach cannot fully take into account the effect of arch vibration into the bridge deck vibration because of its inherent assumptions.

Figure 5 shows the variation of DAF with the speed parameter for a typical case of $\delta_1 = 0.5$, $\delta_2 = 0.6$, $\delta_3 = 2.0$ and $\delta_4 = 1.0$. The variation indicates that the DAF does not necessarily increase with the increase in speed.

The variation of DAF with h/L (rise/span) ratio of the arch bridge is shown in Fig. 6 for two different speeds of the load (keeping the span length and other properties of the bridge unchanged). It is seen that the value of DAF, generally increases with the increase of the h/L ratio, i.e. DAF is greater for a steeper arch bridge.

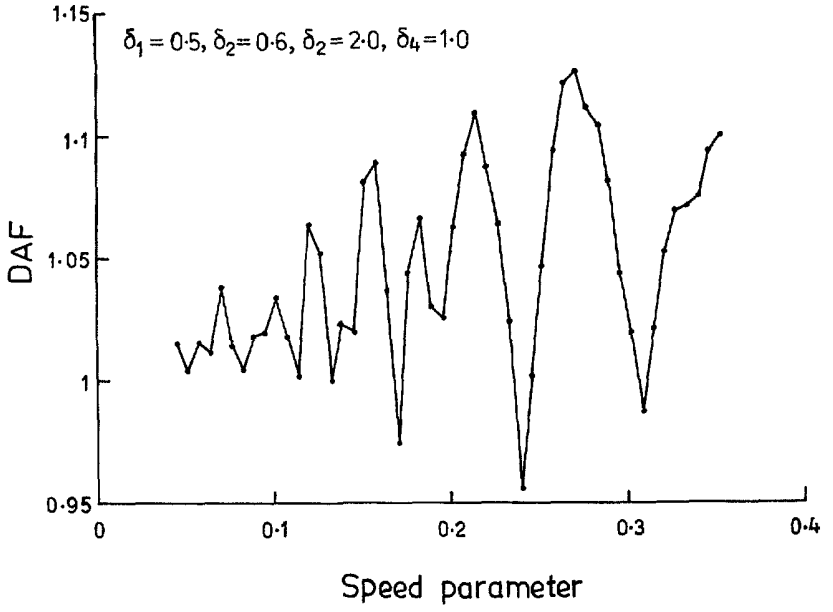

Fig. 5. Variation of DAF with the speed parameter.

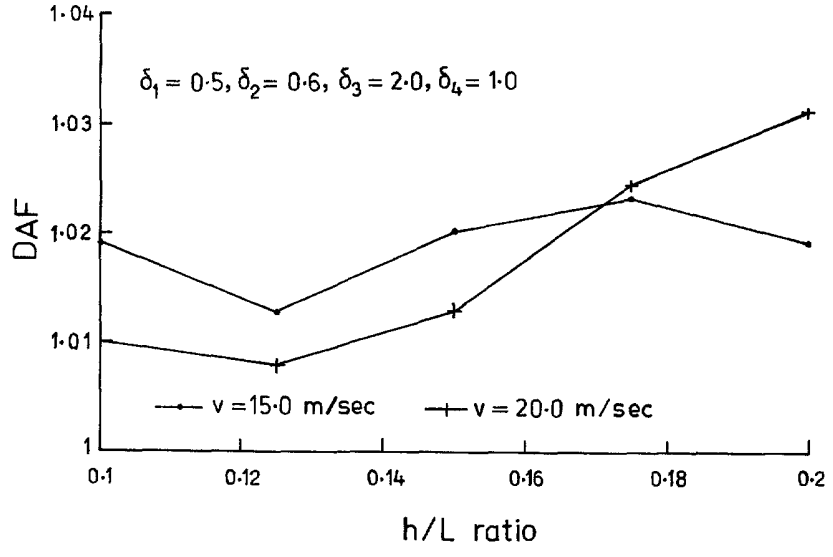

Fig. 6. Variation of DAF with the h/L ratio of arch.

6. CONCLUSIONS

The following conclusions can be drawn from the results of the above investigations.

(i) The comparison of the results obtained from the continuum and lumped mass approaches show that results agree well for certain combinations of the parameters δ_1 to δ_4. For a rigid arch supporting a relatively flexible deck, the values of natural frequencies computed from the two methods show good agreement.

(ii) For a relatively flexible arch compared to the deck, the natural frequencies obtained from the two methods vary by different degrees. Generally, for lower values of δ_1, δ_2 and δ_3 and higher values of δ_4, these differences are less.

(iii) Despite the inherent limitation of the continuum idealization of the arch bridge, the continuum approach predicts fairly well the dynamic behaviour of the bridge deck for certain combinations of the parameters δ_1–δ_4 denoting a relatively flexible deck.

(iv) The variation of DAF with the speed parameter shows that a fluctuating pattern with higher peaks is generally obtained for higher speed parameters.

(v) DAF, generally, increases with increasing h/L ratio of arch. Keeping all other parameters the same, DAF is greater for a steeper arch bridge.

REFERENCES

Bathe, K. J. and Wilson, E. L. (1987). *Numerical Methods in Finite Element Analysis*. Prentice-Hall, New Delhi.

Chatterjee, P. K., Datta, T. K. and Surana, C. S. (1994). Vibration of continuous bridges under moving vehicles. *J. Sound Vibr.* **169**(2), 619–632.

Dusseau, R. A. and Wen, R. K. (1989). Seismic response of deck-type arch bridges. *Earthquake Engng Struct. Dynamics* **18,** 701–715.

Hayashikawa, T. and Watanabe, N. (1981). Dynamic behaviour of continuous beams with moving loads. *J. Engng Mech. ASCE* **107**(EM1), 229–246.

Lee, B. K. and Wilson, J. F. (1989). Free vibration of arches with variable curvature. *J. Sound Vibr.* **136**(1), 75–89.

Nair, R. S. (1986). Buckling and vibration of arches and tied arches. *J. Struct. Engng ASCE* **112**(6), 1429–1440.

Raithel, A. and Franciosi, C. (1984). Dynamic analysis of arches using Lagrangian approach. *J. Struct. Engng ASCE* **110**(4), 847–858.

Wu, J. S. and Lin, T. L. (1990). Free vibration analysis of a uniform cantilever beam with point masses by an analytical–numerical combined method. *J. Sound Vibr.* **136,** 201–213.

Dynamics of steel elevated guideways—an overview (1985). *J. Struct. Engng ASCE* **111**(9), 1873–1898.